DOI: 10.1002/ange.201107394

Lithium Batteries

Double-Structured $LiMn_{0.85}Fe_{0.15}PO_4$ Coordinated with $LiFePO_4$ for Rechargeable Lithium Batteries**

Seung-Min Oh, Seung-Taek Myung, Jin Bum Park, Bruno Scrosati, Khalil Amine, and Yang-Kook Sun**

Olivine-type $LiFePO_4$, discovered by Goodenough and co-workers,[1] has been extensively studied owing to its low costs, environmental friendliness, and in particular, superior thermal stability at the deeply charged state.[2] Use of a carbon coating significantly improved the intrinsic poor electric conductivity, to around $10^{-1}\,S\,cm^{-1}$ from around $10^{-8}\,S\,cm^{-1}$ at room temperature,[3,4] and therefore, this material has undergone intensive investigation for large-scale lithium battery applications.

$LiMnPO_4$, which is an isomorph of $LiFePO_4$, is a more promising electrode material than $LiFePO_4$ as a result of its higher operation voltage (4.1 V vs. Li/Li^+).[5–10] However, $LiMnPO_4$ also suffers from poor electronic conductivity ($< 10^{-10}\,S\,cm^{-1}$) and cycle life because of Mn dissolution, like a Mn spinel.[8]

High energy density is required for mid- to large-scale batteries because the mounting spaces are quite small for vehicles and other energy storage applications. This constraint necessitates use of micron-sized particles to yield high volumetric energy density and reliable battery performance. The few published works that have dealt with micron-sized $LiMnPO_4$ compounds have indicated that the resulting electrochemical properties still need to be improved.[11,12]

We predict that substantial improvement could be overcome by applying a thick and uniform olivine $LiFePO_4$ layer onto micron-sized spherical $LiMn_{0.85}Fe_{0.15}PO_4$ to enhance the cycle life and rate capability (see Scheme 1). Figure S1 a in the Supporting Information shows a schematic drawing of the steps involved in the fabrication of micron-sized $LiMn_{0.85}Fe_{0.15}PO_4$ followed by $LiFePO_4$ surface modification.

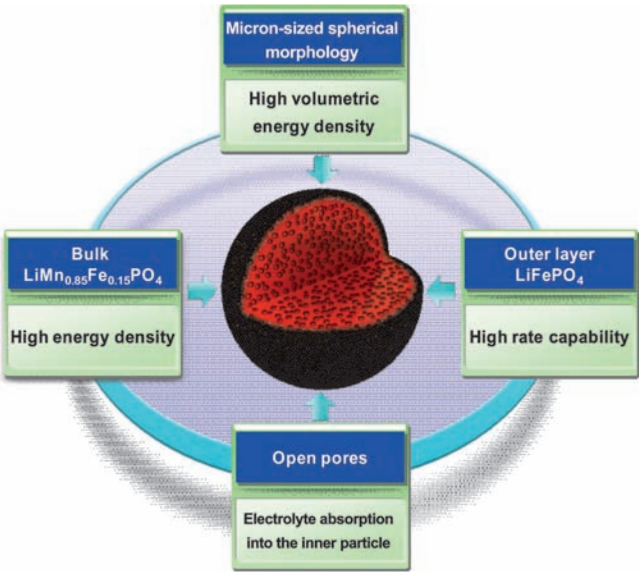

Scheme 1. Double-structured micron-sized $LiMn_{0.85}Fe_{0.15}PO_4$ modified with $LiFePO_4$ and the resulting functions of each component.

A $LiMn_{0.85}Fe_{0.15}PO_4$ particle modified by a $LiFePO_4$ layer (thickness of 0.5 μm) was cross-sectioned by a focused ion beam cut (Figure 1 a). The microscopic images indicate numerous pores in both the bulk and outer layer (Figures 1 b and 1 c). The primary particles seem to agglomerate more densely in the outer layer than the particle bulk because of the smaller particle size of $LiFePO_4$ (Figure 1 c).

A relatively thick carbon layer, which is seen on the outer layer, is mainly associated with carbonization of ascorbic acid and pitch (Figure 1 d). The bulk and outer layer are apparently divided by the interface, and formation of $LiFePO_4$ in the bulk and $LiMnPO_4$ in the outer layer does not likely occur, as indicated by the EPMA result (see Figure S1 d in the Supporting Information). The carbon covers the primary particles in both bulk and outer layer and the surface of the outer layer at the decades of nanometer level. The EELS image also indicates an open network of interconnected nanosized pores distributed throughout the interior of the particles.

---

[*] J. B. Park, Prof. B. Scrosati, Prof. Y.-K. Sun
Department of WCU Energy Engineering, Hanyang University
17 Haengdang-dong, Seongdong-gu, Seoul 133-791 (South Korea)
Prof. S.-T. Myung[+]
Faculty of Nanotechnology
and Advanced Materials Engineering, Sejong University
98 Gunja-dong, Gwnagjin-gu, Seoul 143-747 (South Korea)
Dr. K. Amine
Electrochemical Technology Program, Chemical Sciences
and Engineering Division, Argonne National Laboratory
9700 South Cass Avenue, Argonne, IL 60439 (USA)
Prof. B. Scrosati
Department of Chemistry, University of Rome Sapienza
00185 Rome (Italy)
S.-M. Oh,[+] Prof. Y.-K. Sun
Department of Chemical Engineering, Hanyang University
17 Haengdang-dong, Seongdong-gu, Seoul 133-791 (South Korea)

[+] These authors contributed equally to this work.

[**] This work was supported by the National Research Foundation of Korea (NRF) grant funded by the Korea government (MEST) (grant number 2009-0092780).

Supporting information for this article including experimental details is available on the WWW under http://dx.doi.org/10.1002/anie.201107394.

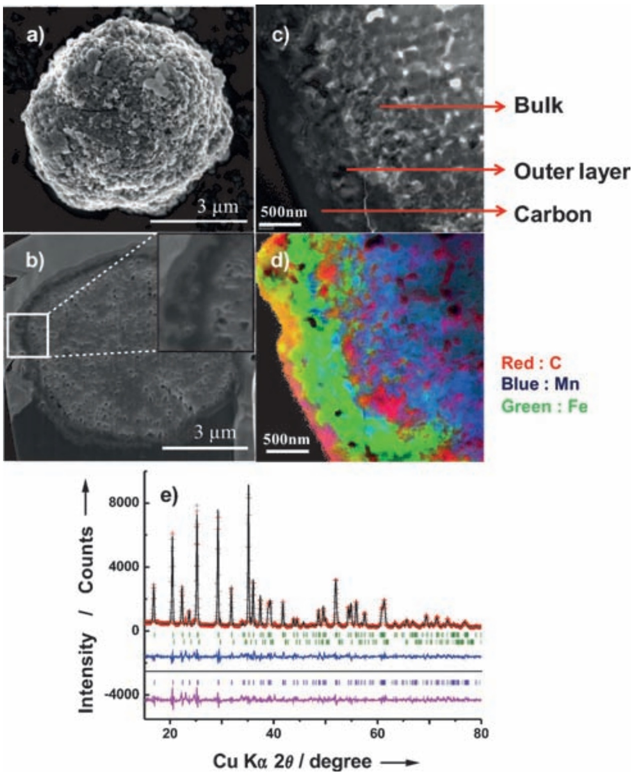

Figure 1. SEM images of a) double-structured $LiMn_{0.85}Fe_{0.15}PO_4$–$LiFePO_4$ (outer layer thickness 0.5 µm) and b) its cross-sectional image obtained from a focused ion beam. c) Cross-sectional TEM image of the magnified part shown in Figure 2b and d) the corresponding EELS image. e) Rietveld refinement of powder XRD patterns of the double-structured $LiMn_{0.85}Fe_{0.15}PO_4$–$LiFePO_4$ (outer layer thickness 0.5 µm; + observed, | Bragg peak position two phases, | Bragg peak position one phase, — calculated, — difference two phases, and — difference one phase).

We next performed Rietveld refinement of the thermally lithiated products (outer layer thickness of 0.5 µm), assuming an average composition of single-phase $LiMn_{0.65}Fe_{0.35}PO_4$ and double-phase $LiMn_{0.85}Fe_{0.15}PO_4$–$LiFePO_4$ based on *Pnma* space group. As a result, two-phase refinement gave a smaller intensity in the difference between the observed and calculated patterns and a better reliability factor (R_{wp}, 12.9 %) than the one-phase (R_{wp}, 16.5 %) refinement (Figure 1e). The two-phase refinement also shows that the double-structured particle is composed of 76 % $LiMn_{0.85}Fe_{0.15}PO_4$ bulk material and 24 % $LiFePO_4$ outer layer material. The calculated lattice parameters for the $LiMn_{0.85}Fe_{0.15}PO_4$ bulk material and $LiFePO_4$ outer layer material agree with reported values (see Table S1 in the Supporting Information).[12,13]

The amount of carbon was determined to be about 2.9 wt %, and the resulting electric conductivity was 7.9×10^{-2} S cm^{-1} at room temperature, which is close to the reported value for $LiFePO_4$.[12] The measured tap density was 1.5 g cm^{-3}, which is the highest value ever achieved in $LiMnPO_4$-related compounds. This feature supports the validity of our synthesis approach that leads to carbon-coated $LiMn_{0.85}Fe_{0.15}PO_4$/$LiFePO_4$ double-structured (hereafter referred to as "LMP/LFP") particles with microscale spherical morphology.

As shown in Figure 2a, a striking feature is that the surface modified LMP/LFP electrode delivered the highest charge and discharge capacity, approximately 152 mAh g^{-1}, and the capacity in the constant current (CC) region on charge is the smallest among the electrodes tested. The presence of carbon-coated $LiFePO_4$ constituting the outer layer, which intrinsically has better electric conductivity than $LiMnPO_4$, is likely to improve the electric conductivity of the double-structured particles further, as evidenced in the CC region on charge. This improvement, in turn, would lead to a higher capacity as a result of lowering the Li^+ diffusion barrier in the LMP/LFP particle. This finding confirms that the surface-modified LMP/LFP sample is not a simple mixture

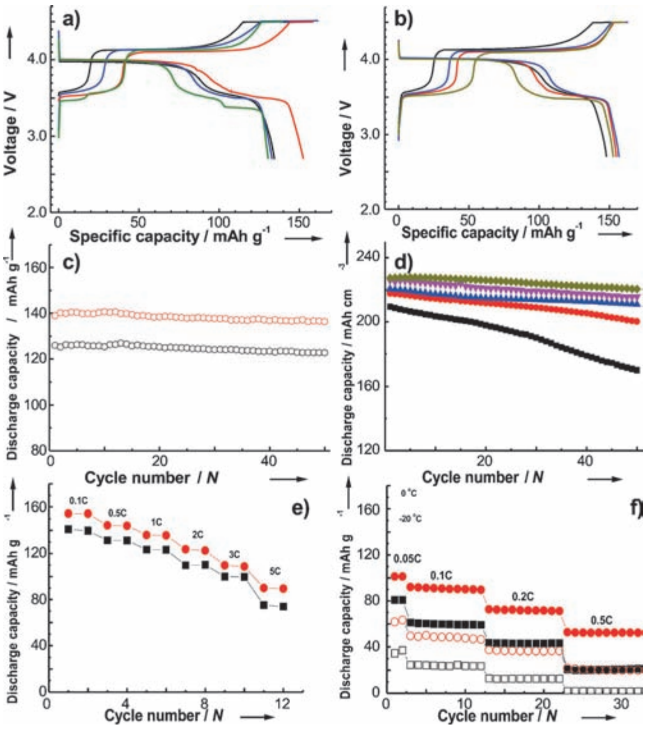

Figure 2. The first charge and discharge profiles of a) bulk $LiMn_{0.85}Fe_{0.15}PO_4$ (—), $LiMn_{0.67}Fe_{0.33}PO_4$ (—), double-structured $LiMn_{0.85}Fe_{0.15}PO_4$–$LiFePO_4$ (—; outer layer thickness of 0.5 µm, $LiMn_{0.65}Fe_{0.35}PO_4$, which is an average composition of the double-structured $LiMn_{0.85}Fe_{0.15}PO_4$–$LiFePO_4$, and a mixture of $LiMn_{0.85}Fe_{0.15}PO_4$–$LiFePO_4$ (—; 76:24 in weight) at 25 °C, b) as a function of the outer layer thickness (— bulk, — 0.2 µm, — 0.5 µm, and — 0.8 µm) at 60 °C measured with a current density of 8.5 mA g^{-1} (0.05 C rate, charge) and 17 mA g^{-1} (0.1 C rate, discharge) in a voltage range of 2.7–4.5 V. c) Cycling stability of bulk $LiMn_{0.85}Fe_{0.15}PO_4$ (○) and double-structured $LiMn_{0.85}Fe_{0.15}PO_4$–$LiFePO_4$ (○, outer layer thickness 0.5 µm) at 25 °C, and d) as a function of outer layer thickness (■ bulk, ● 0.2 µm, ▲ 0.3 µm, ▼ 0.5 µm, and ◆ 0.8 µm) at 60 °C measured with a current density of 85 mA g^{-1} (0.5 C rate) in a voltage range of 2.7–4.5 V. e) Comparison of the rate capability at 25 °C (■ bulk, ● double-structured, outer layer thickness of 0.5 µm) and f) cycling stability at low temperature for bulk $LiMn_{0.85}Fe_{0.15}PO_4$ (■ at 0 °C and □ at −20 °C) and double-structured $LiMn_{0.85}Fe_{0.15}PO_4$–$LiFePO_4$ (outer layer thickness 0.5 µm ● at 0 °C and ○ at −20 °C) charged with a current density of 8.5 mA g^{-1} (0.05 C rate)

but a compound of $LiMn_{0.85}Fe_{0.15}PO_4$ bulk material interfaced with a $LiFePO_4$ outer layer material which perform their functions separately. As anticipated, growth of the $LiFePO_4$ layer thickness diminished the capacity in the 4 V region but increased the capacity at 3.5 V on charge and discharge at 60 °C (Figure 2b). Interestingly, the LMP/LFP electrode shows only 5 mA h g^{-1} of additional capacity relative to the capacity achieved at 25 °C. It is likely that the coordination of $LiMnPO_4$ by the $LiFePO_4$ outer layer improves the electric conductivity and thus yields much higher capacity.

A cycling test at 85 mA g^{-1} (0.5 C rate) showed the excellent capacity retention of olivine compounds at 25 °C (Figure 2c). Even for a full cell using graphite as an anode (see Figure S7 in the Supporting Information), the double-structured LMP/LFP showed the same tendency as high as the half-cell test. However, the bulk material, $LiMn_{0.85}Fe_{0.15}PO_4$, could not maintain the capacity as the LMP/LFP electrode did. Furthermore, the harsh test condition, cycling at 60 °C, seems to be detrimental for the $LiMn_{0.85}Fe_{0.15}PO_4$ electrode (80 % retention of its initial capacity). By contrast, the LMP/LFP electrodes showed excellent capacity retention (outer layer thickness of 0.3–0.8 μm), over 97 % of the initial capacity. Converting to volumetric capacity (240 mA h cm^{-3}), the capacity recorded was remarkably high in the $LiMnPO_4$-based system. Similar to the spinel $LiMn_2O_4$ compound, the capacity fade of the $LiMnPO_4$ system is related to divalent Mn dissolution during operation (4.1 V vs. Li/Li$^+$). Both the elevated temperature (60 °C) and the higher operation voltage accelerate the breakdown of the electrolyte salt, $LiPF_6$, and the formed by-product, HF, can readily decompose the active material. Obviously, dissolution of transition metals takes place for the fully charged bulk and LMP/LFP electrodes (see Figure S8 in the Supporting Information). However, the LMP/LFP material suffered less from the dissolution because of the presence of the $LiFePO_4$ outer layer, which has relatively strong resistivity to HF.[14] Thus, the double-structured LMP/LFP electrode enabled to deliver higher capacity upon cycling at 60 °C.

Although the tested electrodes are composed of micron-sized particles, both electrodes show an impressive rate capability (Figure 2e). At the 5 C rate (850 mA g^{-1} correspond to discharge of entire capacity within 12 min), the LMP/LFP electrode delivered 90 mA h g^{-1}. Even at low temperatures (0 and −20 °C), the LMP/LFP electrode delivered high capacity with good capacity retention (Figure 2f and Figure S8 in the Supporting Information). We believe that the particular morphology of our micron-sized LMP/LFP material bestows upon the electrode high conductivity, facile electrolyte absorption through the open pores, and stability of the $LiFePO_4$ outer layer at high voltage, and this morphology accounts for its observed high capacity and remarkable rate capability. This unique morphology assures high charge–discharge reversibility over a wide temperature range, from −20 to 60 °C.

Olivine-structured $LiMPO_4$ (M = Fe, Mn) possesses stable thermal and safety properties, as shown in Figure 3. The bulk material, $Li_0Mn_{0.85}Fe_{0.15}PO_4$, showed an exothermic reaction over a wide temperature range (200–350 °C), and the heat generation and exothermic temperature were dependent on the presence of the $LiFePO_4$ outer layer at varying thickness because of its outstanding thermal properties. These preliminary results indicate that the surface-modified LMP/LFP electrodes have better thermal stability and, hence, better safety features than most electrode materials tested in lithium ion battery (LIB) systems.

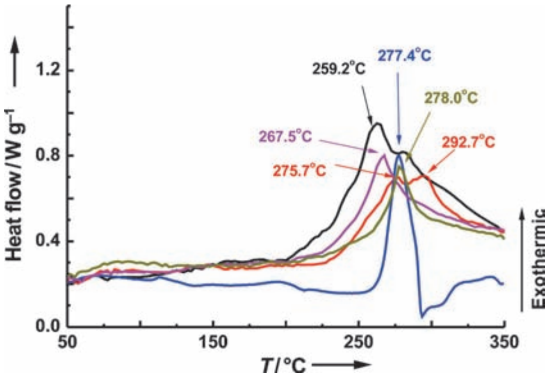

Figure 3. Differential scanning calorimetry traces showing heat flow (216.2, 152.7 J g^{-1}, 108.5 J g^{-1}, 90.3 J g^{-1}, and 70.8 J g^{-1}) from the reaction of the electrolyte with fully charged bulk $Li_0Mn_{0.85}Fe_{0.15}PO_4$ (——), double-structured $LiMn_{0.85}Fe_{0.15}PO_4$–$LiFePO_4$ with varying outer layer thickness of 0.2 (——), 0.5 (——), and 0.8 μm (——), and $LiFePO_4$ (——).

The above results confirm the feasibility of the new concept of $LiMn_{1-x}Fe_xPO_4$ materials (double-structured LMP/LFP chemistry) with varying $LiFePO_4$ outer layer thickness on a $LiMn_{0.85}Fe_{0.15}PO_4$ bulk material for practical LIB systems through fine-tuning of physical characteristics such as tap density, porosity, and spherical morphology. The high tap density (1.5 g cm^{-3}) with spherical morphology also leads to the greatest volumetric energy density (970 Wh m^{-3}) of any $LiMn_{1-x}Fe_xPO_4$ electrode. This system has shown specific discharge capacity approaching the theoretical limit, stable cyclability even at 60 °C, excellent performance at low temperatures, and exceptionally high tap density. We believe that our new LMP/LFP material has nearly ideal properties for achieving successful adaptation in rechargeable lithium cells directed to vehicle and energy storage applications.

Received: October 20, 2011

Keywords: cathode materials · electrochemistry · electrodes · lithium batteries · olivine

---

[1] A. K. Padhi, K. S. Nanjundaswamy, J. B. Goodenough, *J. Electrochem. Soc.* **1997**, *144*, 1188.
[2] S.-Y. Chung, J. T. Bloking, Y.-M. Ching, *Nat. Mater.* **2002**, *1*, 123.
[3] H. Huang, S. C. Yin, L. F. Nazar, *Electrochem. Solid-State Lett.* **2001**, *4*, A170.
[4] Z. Chen, J. R. Dahn, *J. Electrochem. Soc.* **2002**, *149*, A1184.
[5] A. Yamada, Y. Kudo, K.-Y. Liu, *J. Electrochem. Soc.* **2001**, *148*, A747.
[6] T. Shiratsuchi, S. Okada, T. Doi, J. Yamaki, *Electrochim. Acta* **2009**, *54*, 3145.

[7] C. Delacourt, L. Laffont, R. Bouchet, C. Wurm, J.-B. Leriche, M. Morcrette, J.-M. Tarascon, C. Masquelier, *J. Electrochem. Soc.* **2005**, *152*, A913.

[8] M. Yonemura, A. Yamada, Y. Takei, N. Sonoyama, R. Kanno, *J. Electrochem. Soc.* **2004**, *151*, A1352.

[9] S. K. Martha, B. Markovsky, J. Grinblat, Y. Gofer, O. Haik, E. Zinigrad, D. Aurbach, T. Drezen, D. Wang, G. Deghenghi, I. Exnar, *J. Electrochem. Soc.* **2009**, *156*, A541.

[10] S. K. Martha, J. Grinblat, O. Haik, E. Zinigrad, T. Drezen, J. H. Miners, I. Exnar, A. Kay, B. Markovsky, D. Aurbach, *Angew. Chem.* **2009**, *121*, 8711 – 8715; *Angew. Chem. Int. Ed.* **2009**, *48*, 8559 – 8563.

[11] Y. Wang, Y. Yang, Y. Yang, H. Shao, *Mater. Res. Bull.* **2009**, *44*, 2139.

[12] S. W. Oh, S.-T. Myung, H. J. Bang, C. S. Yoon, K. Amine, Y.-K. Sun, *Electrochem. Solid-State Lett.* **2009**, *12*, A181.

[13] S.-M. Oh, S. W. Oh, C. S. Yoon, B. Scrosati, K. Amine, Y.-K. Sun, *Adv. Funct. Mater.* **2010**, *20*, 3260.

[14] Z. Li, D. Zhang, F. Yang, *J. Mater. Sci.* **2009**, *44*, 2435.